

Damping of Collective Nuclear Motion and Thermodynamic Properties of Nuclei beyond Mean Field^{*†}

Hong-Gang Luo^{1,2}, W. Cassing¹ and Shun-Jin Wang^{1,2}

1. Institut für Theoretische Physik, Universität Giessen
35392 Giessen, Germany

2. Department of Modern Physics, Lanzhou University,
Lanzhou 730000, PR China

October 12, 2018

Abstract

The dynamical description of correlated nuclear motion is based on a set of coupled equations of motion for the one-body density matrix $\rho(11';t)$ and the two-body correlation function $c_2(12,1'2';t)$, which is obtained from the density-matrix hierarchy beyond conventional mean-field approaches by truncating 3-body correlations. The resulting equations nonperturbatively describe particle-particle collisions (short-range correlations) as well as particle-hole interactions (long-range correlations). Within a basis of time-dependent Hartree-Fock states these equations of motion are solved for collective vibrations of ^{40}Ca at several finite thermal excitation energies corresponding to temperatures $T = 0 - 6$ MeV. Transport coefficients for friction and diffusion are extracted from the explicit solutions in comparison to the solutions of the associated TDHF, VUU, Vlasov or damped quantum oscillator equations of motion. We find that the actual magnitude of the transport coefficients is strongly influenced by particle-hole correlations at low temperature which generate large fluctuations in the nuclear shape degrees of freedom. Thermodynamically, the specific heat and the entropy of the system as a function of temperature does not differ much from the mean-field limit except for a bump in the specific heat around $T \simeq 4$ MeV which we attribute to the melting of shell effects in the correlated system.

PACS: 24.10.Cn; 24.30.Cz; 24.60Ky

Keywords: Many-body theory; Giant resonances; Fluctuation phenomena

^{*}Part of the PhD thesis of Hong-Gang Luo;

[†]supported by DAAD, MFT, and GSI Darmstadt

1 Introduction

The damping of nuclear collective motion and the role of short-range and long-range nuclear correlations [1, 2] in the relaxation still is left as an open problem from the fully microscopic point of view. Whereas at intermediate energy heavy-ion collisions the system is essentially damped by in-medium nucleon-nucleon collisions within the time-dependent mean field [3, 4, 5], the relaxation of giant resonances at low excitation energy appears to be dominated by residual 2 particle – 2 hole (2p-2h) correlations [6, 7] that are not incorporated in standard transport theories [3, 4, 5]. Though the latter approaches have proven to quite reliably describe one-body observables in heavy-ion reactions, they fail in describing fluctuation phenomena like 'multifragmentation'. Thus Langevin forces - that are related to fluctuations in the particle collision number or in momentum space - have been proposed in addition to the Vlasov-Uehling-Uhlenbeck (VUU) dynamics [8] - [18]. Since the various approaches involve quite different assumptions about the dynamical origin and the size of 'fluctuations', a more rigorous analysis within the framework of a nonperturbative quantum two-body theory appears necessary.

More specifically, nuclear giant resonances of hot nuclei have been studied in detail in both experimental [19, 20, 21, 22] and theoretical nuclear physics [23] - [33] to learn about the nuclear collectivity and the lifetime of these modes. The stability of the damping widths against temperature, the effects of shape degrees of freedom on the damping process, the role played by particle-hole (long-range) correlations, and the distinction among the damping processes in different dynamical models have presented open and interesting problems. Though several authors have addressed these problems within various approaches [6, 7, 23, 24, 25, 26, 27, 28, 29, 32, 33, 34, 35, 36, 37], many microscopic aspects remain unclear. It is the purpose of this paper to investigate these problems from a systematical point of view and in a more detailed way especially in a comparison of quantum mechanical and semiclassical approaches.

In Section 2 we briefly review the underlying microscopic approach obtained from the correlation dynamical truncation scheme [38] and present the approximations performed for the actual calculations. Section 3 is devoted to a presentation of the microscopic results in case of isoscalar quadrupole motion of ^{40}Ca and to the extraction of transport coefficients from the mean values and dispersions of the quadrupole operator Q and its time derivative \dot{Q} . The results will also be compared to the mean-field limit TDHF as well as to the semiclassical limits of VUU and solutions based on the Vlasov equation. Furthermore, in Section 4 the specific heat, entropy and free energy of the nucleus ^{40}Ca will be evaluated as a function of temperature in the correlated two-body theory in comparison to the mean-field limit. A summary and discussion in Section 5 concludes this study.

2 Nuclear quantum correlation dynamics (NQCD)

The dynamical description of the nuclear many-body problem in the non-relativistic limit is based on coupled equations of motion for the one-body density matrix $\rho(11'; t)$

and the two-body correlation function $c_2(12, 1'2'; t)$ in the equal time limit [38] - [41];

$$\begin{aligned} i\partial/\partial t \rho(11'; t) &= [t(1) + U(1; t)]\rho(11'; t) - \rho(11'; t)[t(1') + U^\dagger(1'; t)] \\ &\quad + Tr_{(2=2')}[v(12)c_2(12, 1'2'; t) - c_2(12, 1'2'; t)v(1'2')] \end{aligned} \quad (1)$$

where the two-body density matrix is written as $\rho_2(12, 1'2'; t) = \rho_{20}(12, 1'2'; t) + c_2(12, 1'2'; t)$ with $\rho_{20}(12, 1'2'; t) = \mathcal{A}_{12}\rho(11'; t)\rho(22'; t)$. In (1) $t(i)$ denotes the kinetic energy of particle i while $v(ij)$ is the bare two-body interaction. The time evolution of c_2 is determined by

$$\begin{aligned} i\partial/\partial t c_2(12, 1'2'; t) &= [t(1) + t(2) + U(1; t) + U(2; t)]c_2(12, 1'2'; t) \\ &\quad - c_2(12, 1'2'; t)[t(1') + t(2') + U^\dagger(1'; t) + U^\dagger(2'; t)] \\ &\quad + [Q_{12}^- v(12)\rho_{20}(12, 1'2'; t) - \rho_{20}(12, 1'2'; t)v(1'2')Q_{1'2'}^{\dagger-}] \end{aligned} \quad (2)$$

$$+ [Q_{12}^- v(12)c_2(12, 1'2'; t) - c_2(12, 1'2'; t)v(1'2')Q_{1'2'}^{\dagger-}] \quad (3)$$

$$\begin{aligned} &+ Tr_{(3=3')}[v(13)\mathcal{A}_{13}\mathcal{A}_{1'2'} - v(1'3')\mathcal{A}_{1'3'}\mathcal{A}_{12}]\rho(11'; t)c_2(23, 2'3'; t) \\ &+ Tr_{(3=3')}[v(23)\mathcal{A}_{23}\mathcal{A}_{1'2'} - v(2'3')\mathcal{A}_{2'3'}\mathcal{A}_{12}]\rho(22'; t)c_2(13, 1'3'; t) \end{aligned} \quad (4)$$

$$+ Tr_{(3=3')}\{[v(13) + v(23)]c_3(123, 1'2'3'; t) - c_3(123, 1'2'3'; t)[v(1'3') + v(2'3')]\}. \quad (5)$$

In equations (1) - (5) $Tr_{(i=i')}$ stands for a summation over spin $\sigma(i)$ and isospin $\tau(i)$ as well as an integration over d^3r_i with $i = i'$, while \mathcal{A}_{ij} is the antisymmetrization operator for fermions defined by $\mathcal{A}_{ij} = 1 - P_{ij}$ and P_{ij} is the permutation operator between particle i and j . In (1) - (5) we have, furthermore, introduced the mean-field potential

$$U(i; t) = Tr_{(3=3')}\{v(i3)\mathcal{A}_{i3}\rho(33'; t)\} \quad (6)$$

and the Pauli-blocking operator for $p - p$ and $h - h$ interactions

$$Q_{ij}^- = 1 - Tr_{(3=3')}(P_{i3} + P_{j3})\rho(33'; t) \quad (7)$$

In order to close (1) - (5) the three-body correlation term (5) will be dropped in the following. For an explicit discussion of (5) in the context of trace conservation laws we refer the reader to Ref. [41].

2.1 Time-Dependent Density-Matrix Theory (TDDM)

Because of technical limitations the set of coupled equations for the one-body density matrix $\rho(11'; t)$ (1) and the two-body correlation function $c_2(12, 1'2'; t)$ (2) - (4) can, at present, only be solved accurately for moderate excitations of the nuclear system. In this case one can expand both ρ and c_2 in terms of single-particle states ψ_α fulfilling the TDHF equations,

$$(i \frac{\partial}{\partial t} - h(1))\psi_\alpha(1, t) = 0 \quad (8)$$

according to

$$\begin{aligned}\rho(11'; t) &= \sum_{\alpha, \beta} n_{\alpha\beta}(t) \psi_{\beta}^*(1', t) \psi_{\alpha}(1, t) \\ c_2(12, 1'2'; t) &= \sum_{\alpha, \beta, \alpha', \beta'} C_{\alpha\beta\alpha'\beta'}(t) \psi_{\alpha}(1, t) \psi_{\beta}(2, t) \psi_{\alpha'}^*(1', t) \psi_{\beta'}^*(2', t),\end{aligned}\quad (9)$$

where the operator $h(i) = t(i) + U(i)$ in (8) is the one-body hamiltonian, i.e. the sum of a kinetic energy term and the selfconsistent mean field (6) .

The equations of motion for the occupation matrix $n_{\alpha\beta}(t)$ and $C_{\alpha\beta\alpha'\beta'}(t)$ then read [7, 34, 36]

$$i \frac{\partial}{\partial t} n_{\alpha\beta} = \sum_{\gamma\delta\sigma} \{ \langle \alpha\sigma | v | \gamma\delta \rangle C_{\gamma\delta\beta\sigma} - C_{\alpha\delta\gamma\sigma} \langle \gamma\sigma | v | \beta\delta \rangle \} \quad (10)$$

and

$$i \frac{\partial}{\partial t} C_{\alpha\beta\alpha'\beta'} = B_{\alpha\beta\alpha'\beta'} + P_{\alpha\beta\alpha'\beta'} + H_{\alpha\beta\alpha'\beta'}, \quad (11)$$

where

$$\begin{aligned}B_{\alpha\beta\alpha'\beta'} &= \sum_{\lambda_1\lambda_2\lambda_3\lambda_4} \langle \lambda_1\lambda_2 | v | \lambda_3\lambda_4 \rangle_{\mathcal{A}} \\ &\cdot \{ (\delta_{\alpha\lambda_1} - n_{\alpha\lambda_1})(\delta_{\beta\lambda_2} - n_{\beta\lambda_2}) n_{\lambda_3\alpha'} n_{\lambda_4\beta'} - n_{\alpha\lambda_1} n_{\beta\lambda_2} (\delta_{\lambda_3\alpha'} - n_{\lambda_3\alpha'}) (\delta_{\lambda_4\beta'} - n_{\lambda_4\beta'}) \}\end{aligned}\quad (12)$$

represents the lowest order contribution of collisions in the particle-particle channel (Born approximation), while the term P represents the higher order particle-particle (and hole-hole) contributions,

$$\begin{aligned}P_{\alpha\beta\alpha'\beta'} &= \sum_{\lambda_1\lambda_2\lambda_3\lambda_4} \langle \lambda_1\lambda_2 | v | \lambda_3\lambda_4 \rangle [\delta_{\alpha\lambda_1} \delta_{\beta\lambda_2} C_{\lambda_3\lambda_4\alpha'\beta'} - \delta_{\lambda_3\alpha'} \delta_{\lambda_4\beta'} C_{\alpha\beta\lambda_1\lambda_2} \\ &- \delta_{\alpha\lambda_1} n_{\beta\lambda_2} C_{\lambda_3\lambda_4\alpha'\beta'} - \delta_{\lambda_2\beta} n_{\alpha\lambda_1} C_{\lambda_4\lambda_3\beta'\alpha'} + \delta_{\lambda_3\alpha'} n_{\lambda_4\beta'} C_{\alpha\beta\lambda_1\lambda_2} + \delta_{\lambda_4\beta'} n_{\lambda_3\alpha'} C_{\alpha\beta\lambda_1\lambda_2}].\end{aligned}\quad (13)$$

The last term

$$\begin{aligned}H_{\alpha\beta\alpha'\beta'} &= \sum_{\lambda_1\lambda_2\lambda_3\lambda_4} \langle \lambda_1\lambda_2 | v | \lambda_3\lambda_4 \rangle \\ &[\delta_{\alpha\lambda_1} (n_{\lambda_3\alpha'} C_{\beta\lambda_4\beta'\lambda_2} - n_{\lambda_3\beta'} C_{\beta\lambda_4\alpha'\lambda_2} - n_{\lambda_4\alpha'} C_{\lambda_3\beta\lambda_2\beta'} - n_{\lambda_4\beta'} C_{\lambda_3\beta\alpha'\lambda_2}) \\ &+ \delta_{\beta\lambda_2} (n_{\lambda_4\beta'} C_{\alpha\lambda_3\alpha'\lambda_1} - n_{\lambda_4\alpha'} C_{\alpha\lambda_3\beta'\lambda_1} - n_{\lambda_3\beta'} C_{\alpha\lambda_4\alpha'\lambda_1} - n_{\lambda_3\alpha'} C_{\alpha\lambda_4\lambda_1\beta'}) \\ &- \delta_{\beta'\lambda_4} (n_{\beta\lambda_2} C_{\alpha\lambda_3\alpha'\lambda_1} - n_{\alpha\lambda_2} C_{\beta\lambda_3\alpha'\lambda_1} - n_{\beta\lambda_1} C_{\alpha\lambda_3\alpha'\lambda_2} - n_{\alpha\lambda_1} C_{\beta\lambda_3\lambda_2\alpha}) \\ &- \delta_{\alpha'\lambda_3} (n_{\alpha\lambda_1} C_{\beta\lambda_4\beta'\lambda_2} - n_{\alpha\lambda_2} C_{\alpha\lambda_4\beta'\lambda_2} - n_{\alpha\lambda_2} C_{\beta\lambda_4\beta'\lambda_1} - n_{\beta\lambda_2} C_{\alpha\lambda_4\lambda_1\beta'})]\end{aligned}\quad (14)$$

is the contribution to the equations of motion in the particle-hole channel. The set of coupled equations (10) and (11) provides a non-perturbative description of large amplitude nuclear motion denoted as Time-Dependent Density-Matrix (**TDDM**) theory which takes into account collisions among nucleons to all orders in the interaction and thus supersedes the quantum approaches in Refs. [33, 42] that are limited to the Born approximation, i.e. retaining only $B_{\alpha\beta\alpha'\beta'}$ in Eq. (11). We note that the theory fulfills the conservation of particle number, momentum, and energy [34].

2.2 Dispersion of one-body operators

Since TDDM is a consistent two-body theory it allows to evaluate one-body as well as two-body observables. Of specific interest are the mean values and the fluctuation properties of collective one-body operators, for which we give the microscopic expressions. Note that contrary to Refs. [23, 37, 43] no explicit equations of motion for a collective degree of freedom have to be set up since Eqs. (10) and (11) already describe the full dynamics.

The quadrupole operator (as well as any one-body operator O) is defined as

$$O = \sum_{\alpha,\beta} \langle \alpha | O | \beta \rangle a_{\alpha}^{\dagger} a_{\beta}, \quad (15)$$

where a_{α}^{\dagger} and a_{β} are creation and annihilation operators of a nucleon. Our definition of the quadrupole operator $Q_2(\mathbf{r}) \equiv Q(\mathbf{r})$ is explicitly

$$Q(\mathbf{r}) = \frac{1}{2} \sqrt{\frac{5}{4\pi}} (2z^2 - x^2 - y^2) \quad (16)$$

which gives for the time derivative

$$\dot{Q}(\mathbf{r}, \mathbf{p}) = \frac{-i}{\hbar} [Q, h] = \sqrt{\frac{5}{4\pi}} \frac{1}{2m} (2zp_z + 2p_z z - xp_x - p_x x - yp_y - p_y y). \quad (17)$$

The inertia mass operator of the quadrupole motion, $M(\mathbf{r})$, is

$$\frac{1}{M(\mathbf{r})} = -\frac{1}{\hbar^2} [Q(\mathbf{r}), [Q(\mathbf{r}), h]] = -\frac{i}{\hbar} [Q(\mathbf{r}), \dot{Q}(\mathbf{r}, \mathbf{p})] = \frac{5}{4\pi m} (4z^2 + x^2 + y^2). \quad (18)$$

Eq. (18) presents not only an expression for the quadrupole mass operator but also a more general commutation relation for the quadrupole operator $Q(\mathbf{r})$ and its velocity operator $\dot{Q}(\mathbf{r}, \mathbf{p})$, in which the constant $i\hbar$ is replaced by the operator $i\hbar/M(\mathbf{r})$. This is equivalent to a collective momentum operator $P = M(\mathbf{r})\dot{Q}(\mathbf{r}, \mathbf{p})$.

From the commutation relation (18) one can derive the corresponding uncertainty relation as,

$$\sigma_Q^2 \sigma_{\dot{Q}}^2 \geq \left(\frac{\hbar}{2} \left\langle \frac{1}{M(\mathbf{r})} \right\rangle \right)^2, \quad (19)$$

or

$$\sigma_Q^2 M_Q^2 \sigma_{\dot{Q}}^2 \geq \left(\frac{\hbar}{2} \right)^2, \quad (20)$$

with the definition of the quadrupole mass $1/M_Q = \langle 1/M(\mathbf{r}) \rangle$, and with σ_Q^2 and $\sigma_{\dot{Q}}^2$ defined by Eq. (22) below. Eq. (20) will be checked as a boundary condition in our following numerical calculations explicitly.

The mean value and the dispersion of a one-body operator O are given by:

$$\langle O \rangle = \sum_{\alpha,\beta} \langle \alpha | O | \beta \rangle \langle a_{\alpha}^{\dagger} a_{\beta} \rangle = \sum_{\alpha,\beta} \langle \alpha | O | \beta \rangle n_{\beta\alpha} \quad (21)$$

$$\begin{aligned}
\sigma_O^2 &= \sum_{\alpha,\alpha',\beta,\beta'} \langle \alpha|O|\beta \rangle \langle \alpha'|O|\beta' \rangle \langle a_\alpha^+ a_\beta a_\alpha^+ a_{\beta'} \rangle - \langle O \rangle^2 \\
&= \sum_{\alpha,\alpha',\beta,\beta'} \langle \alpha|O|\beta \rangle \langle \alpha'|O|\beta' \rangle (\delta_{\alpha'\beta} \langle a_\alpha^+ a_{\beta'} \rangle + \langle a_\alpha^+ a_\alpha^+ a_{\beta'} a_{\beta'} \rangle) - \langle O \rangle^2 \\
&= \sum_{\alpha,\beta,\beta'} \langle \alpha|O|\beta \rangle \langle \beta|O|\beta' \rangle n_{\beta'\alpha} + \sum_{\alpha,\alpha',\beta,\beta'} \langle \alpha|O|\beta \rangle \langle \alpha'|O|\beta' \rangle (C_{\beta\beta'\alpha\alpha'} - n_{\beta\alpha'} n_{\beta'\alpha}) \\
&= \sum_{\alpha,\beta'} \langle \alpha|O^2|\beta' \rangle n_{\beta'\alpha} + \sum_{\alpha,\alpha',\beta,\beta'} \langle \alpha|O|\beta \rangle \langle \alpha'|O|\beta' \rangle (C_{\beta\beta'\alpha\alpha'} - n_{\beta\alpha'} n_{\beta'\alpha}), \quad (22)
\end{aligned}$$

where the matrix elements $n_{\alpha\beta}$ and $C_{\alpha\beta\alpha'\beta'}$ depend on time explicitly. In case of TDHF we simply have $C_{\beta\beta'\alpha\alpha'} = 0$ and $n_{\alpha\beta} = \delta_{\alpha\beta} n_\alpha$ where n_α denotes the occupation probability of the single-particle state ψ_α . This gives

$$\langle O \rangle = \sum_{\alpha} \langle \alpha|O|\alpha \rangle n_\alpha, \quad (23)$$

$$\begin{aligned}
\sigma_O^2 &= \sum_{\alpha,\beta} \langle \alpha|O|\beta \rangle (1 - n_\beta) \langle \beta|O|\alpha \rangle n_\alpha \\
&= \sum_{\alpha} \langle \alpha|O^2|\alpha \rangle n_\alpha - \sum_{\alpha,\beta} \langle \alpha|O|\beta \rangle \langle \beta|O|\alpha \rangle n_\beta n_\alpha. \quad (24)
\end{aligned}$$

We note that the summation over β in the first terms of Eqs. (22) and (24) should be taken in the whole Hilbert space ($\sum_{\beta} |\beta \rangle \langle \beta| = 1$) so that it yields an identity in the whole Hilbert space. This observation is important since the numerical calculations are carried out in a truncated Hilbert space.

2.3 Technical approximations

In our actual calculations we approximate the interaction v appearing in the mean-field potential (6) by a Bonche-Koonin-Negele (BKN) [44] force and use $v(12) = V_0 \delta(\mathbf{r}_1 - \mathbf{r}_2)$ for the residual interaction appearing in (12)-(14) with $V_0 = -300 \text{ MeV fm}^3$ for technical reasons (see below) as in Refs. [7, 36, 45]. We have solved the coupled equations (10) and (11) for the case of the isoscalar monopole or quadrupole vibration of ^{40}Ca as a function of temperature since the dipole mode was found in Ref. [7] to be dominated by mean-field dynamics. To carry out calculations at various temperatures we describe the initial occupation numbers by appropriate Fermi distributions (characterized by a temperature T) and propagate the system in time. The set of single-particle levels used in the calculations include the 1s, 1p, 2s, 1d, 2p, and 1f shell. The correlated state, which is generated by an adiabatic switching on of the residual interaction [45, 46], is then boosted at a certain time (typically after $2 \cdot 10^{-22} \text{ s}$) by applying appropriate phase factors to the wavefunctions ψ_β proportional to a strength factor α . In this way the system acquires a well defined collective energy proportional to α^2 . The set of equations (8) - (11) is then integrated in time with timestep-size $\Delta t = 0.5 \cdot 10^{-23} \text{ s}$. We note that the total energy and number of particles are conserved well throughout the timescales of interest here.

2.4 Specific heat, entropy, and free energy

The energy of the system reads for the present Skyrme interaction as well as the residual δ -interaction:

$$\begin{aligned}
E = \int \epsilon(\mathbf{r}) d^3\mathbf{r} = \int d^3r & \left[\frac{\hbar^2}{2m}(\tau_n + \tau_p) + \frac{t_0}{2}(2\rho_n\rho_p + \frac{1}{2}(\rho_n^2 + \rho_p^2)) \right. \\
& + \frac{t_3}{4}(\rho_n^2\rho_p + \rho_n\rho_p^2) \left. \right] + \frac{v_L}{2}[E_y(\rho_n, \rho_n) + E_y(\rho_p, \rho_p)] + v_U E_y(\rho_n, \rho_p) \\
& + \frac{e^2}{2} \int \int d^3\mathbf{r} d^3\mathbf{r}' \frac{\rho_p(\mathbf{r})\rho_p(\mathbf{r}')}{|\mathbf{r} - \mathbf{r}'|} + \frac{V_0}{2} \int C_2(\mathbf{r}, \mathbf{r}; \mathbf{r}, \mathbf{r}) d^3\mathbf{r}, \tag{25}
\end{aligned}$$

where

$$E_y(\rho_q, \rho_{q'}) = \int \int d^3\mathbf{r} d^3\mathbf{r}' \frac{\exp(-\mu |\mathbf{r} - \mathbf{r}'|)}{\mu |\mathbf{r} - \mathbf{r}'|} \rho_q(\mathbf{r})\rho_{q'}(\mathbf{r}') \tag{26}$$

results from the finite range Yukawa force [44]. The total energy of the system - after adiabatically switching on the residual interactions - depends on the initial thermal excitation energy characterized by a temperature T , from which one can calculate numerically the specific heat as

$$C_v(T) = \frac{\partial E(T)}{\partial T}. \tag{27}$$

The entropy for the many-body system, which should not be mixed up with the one-body entropy, then is given by

$$S(T) = \int_0^T \frac{C_v(T')}{T'} dT' \tag{28}$$

and the free energy follows as

$$F(T) = E - TS. \tag{29}$$

Furthermore, the fluctuation in energy of the system can be evaluated as,

$$\sigma_H^2 = \langle (H - \langle H \rangle)^2 \rangle = \langle H^2 \rangle - E^2 = T^2 C_v, \tag{30}$$

which can be considered as an order parameter for a phase transition.

2.5 The semiclassical limit

As shown in detail in Ref. [4] the coupled equations of motion (1) - (3), i.e. excluding (4), transform to a Vlasov-Uehling-Uhlenbeck (VUU) equation in the semiclassical limit when adopting an on-shell (Markov) approximation for the NN -interactions and expanding up to the first order in the derivative operator $\hbar^{-1}\nabla_r \cdot \nabla_p$ with respect to the particle phase-space variables \mathbf{r} and \mathbf{p} . This gives the familiar VUU equation (for momentum-independent mean-fields)

$$\left\{ \frac{\partial}{\partial t} + \frac{\mathbf{p}}{E} \cdot \nabla_r - \nabla_r U(\mathbf{r}) \cdot \nabla_p \right\} f(\mathbf{r}, \mathbf{p}; t) = I_{coll}(\mathbf{r}, \mathbf{p}; t), \tag{31}$$

where the collision term is given by [4]

$$\begin{aligned}
I_{coll}(\mathbf{r}, \mathbf{p}; t) &= \frac{4}{(2\pi)^3} \int d^3 p_2 \int d\Omega |v_{12}| \frac{d\sigma}{d\Omega}(\mathbf{p}, \mathbf{p}_2) \\
&\times (f(\mathbf{r}, \mathbf{p}_3; t) f(\mathbf{r}, \mathbf{p}_4; t) (1 - f(\mathbf{r}, \mathbf{p}; t)) (1 - f(\mathbf{r}, \mathbf{p}_2; t)) \\
&- f(\mathbf{r}, \mathbf{p}; t) f(\mathbf{r}, \mathbf{p}_2; t) (1 - f(\mathbf{r}, \mathbf{p}_3; t)) (1 - f(\mathbf{r}, \mathbf{p}_4; t))). \tag{32}
\end{aligned}$$

In Eq. (32) $d\sigma/d\Omega$ denotes the differential cross section for the on-shell scattering process $1 + 2 \rightarrow 3 + 4$ while $|v_{12}|$ is the relative velocity of the colliding nucleons; the outgoing momenta \mathbf{p}_3 and \mathbf{p}_4 are fixed by energy- and momentum conservation except for the scattering angle Ω in their center-of-mass. When neglecting the collision term (32), the Vlasov equation (31) is equivalent to the statement, that the total time derivative of the one-body phase-space density $f(\mathbf{r}, \mathbf{p}; t)$ vanishes, i.e $d/dt f = 0$. The Vlasov equation thus corresponds to the semiclassical limit of TDHF. The VUU equation (31) is conventionally [3, 4] solved within the testparticle method and has been exploited extensively for the nonequilibrium description of proton-nucleus or nucleus-nucleus collisions at intermediate [4] and high energies [47]. Here we will compare the results of the semiclassical VUU or Vlasov equation with those for the quantum mechanical theories TDDM and TDHF, respectively.

2.6 The damped harmonic oscillator in quantum physics

For later comparison and interpretation of the numerical results we recall the equations of motion for a damped harmonic quantum oscillator (QHO) with respect to fluctuations in the collective coordinates Q and \dot{Q} (cf. Refs. [23, 37, 43]):

$$\frac{d}{dt} \sigma_Q^2 = 2\sigma_{Q\dot{Q}} \tag{33}$$

$$\frac{d}{dt} \sigma_{Q\dot{Q}} = -2\gamma_Q \sigma_{Q\dot{Q}} + \frac{\Omega^2}{M_Q} \sigma_Q^2 \tag{34}$$

$$\frac{d}{dt} \sigma_{\dot{Q}}^2 = -2\gamma_Q \sigma_{\dot{Q}}^2 + \frac{\Omega^2}{M_Q} \sigma_{Q\dot{Q}} + D_{QQ}(T), \tag{35}$$

where the fluctuations are defined as

$$\begin{aligned}
\sigma_Q^2 &= \langle Q^2 \rangle - \langle Q \rangle^2; \\
\sigma_{Q\dot{Q}} &= \langle Q\dot{Q} \rangle - \langle Q \rangle \langle \dot{Q} \rangle; \\
\sigma_{\dot{Q}}^2 &= \langle \dot{Q}^2 \rangle - \langle \dot{Q} \rangle^2. \tag{36}
\end{aligned}$$

In Eq. (34) Ω denotes the collective frequency, γ_Q a collective friction coefficient, M_Q the collective mass parameter, whereas $D_{QQ}(T)$ is the diffusion coefficient given by

$$D_{QQ}(T) = \frac{\hbar\Omega\gamma_Q}{M_Q} \coth \frac{\hbar\Omega}{2T}. \tag{37}$$

Note that only for large temperatures $T \gg \hbar\Omega$ the Einstein relation

$$D_{QQ} = 2\gamma_Q T/M_Q \quad (38)$$

is obtained. In view of (small amplitude) nuclear collective quadrupole motion we have $T < \hbar\Omega$ such that relation (38) does not apply. When using $P \equiv M_Q \dot{Q}$ instead of \dot{Q} the diffusion coefficient (37) or (38) picks up an additional factor M_Q^2 .

3 Numerical results

As a first test we study the 'hole-strength' distribution of ^{40}Ca within the nonperturbative limit TDDM by integrating the coupled equations (8), (10), and (11) in time with the initial condition $C_{\alpha\beta\alpha'\beta'} = 0$, which corresponds to the respective Hartree-Fock groundstate. The correlated state is then generated in line with the Gell-Mann-Low theorem by adiabatically switching on the residual interaction as

$$V(t) = V_0 [1 - \exp(-t/\tau)], \quad (39)$$

where $\tau \simeq 5 \cdot 10^{-22} \text{sec}$ was found to be sufficiently large to achieve convergence (cf. also Ref. [45]). The numerical solutions for the occupation numbers $n_\alpha(t)$ deviate from 0 and 1 and slightly oscillate in time. By averaging over time (for $t \geq 10^{-21} \text{sec}$) we obtain average occupation numbers $\langle n_\alpha \rangle$ which are shown in Fig. 1 as a function of the time-averaged single-particle energies ϵ_α . The solid line presents a smooth fit through the discrete points for orientation. The latter one is remarkably close to the experimental data from Ref. [48] which indicates that the proper strength of the residual correlations is well described by TDDM for $V_0 = -300 \text{ MeV fm}^3$, which we consider as fixed from now on.

We note in passing that the average occupation numbers have no direct counterpart in the semiclassical limit since the s.p. energy does not enter the VUU equation explicitly, but only its space- and momentum derivatives. In analogy to the mean-field limit the nucleon phase-space distribution at $T = 0$ is given by a local Thomas-Fermi distribution (for fixed spin and isospin)

$$f_0(\mathbf{r}, \mathbf{p}; t) = \Theta(p_F(\mathbf{r}) - |\mathbf{p}|) \quad (40)$$

with

$$p_F(\mathbf{r}) = \left(\frac{3}{2}\pi\rho(\mathbf{r})\right)^{1/3} \quad (41)$$

where $\rho(\mathbf{r})$ denotes the nucleon density distribution.

3.1 Damping of giant quadrupole motion

Whereas in mean-field theory the frequency of collective modes can be rather well determined, its damping width appears to be dominated by higher order NN interactions. As was found in Ref. [7] the role of $2p - 2h$ matrix elements is very pronounced for giant quadrupole motion, which we analyse here in more detail.

The time evolution of the quadrupole moment $Q(t)$ and that of $\dot{Q}(t)$ - which carries a similar information - are presented in Figs. 2 and 3 for TDHF (upper parts) and TDDM (lower parts) for an isoscalar quadrupole excitation of 20 MeV of ^{40}Ca at an initial temperature of $T=1, 3, \text{ and } 5$ MeV.

Whereas there is only small damping in the case of TDHF, the collective motion is strongly damped in the limit TDDM demonstrating the decisive role of residual NN interactions.

The questions arises, to what extent the damping of the quadrupole motion can be attributed to on-shell particle-particle collisions as inherent in the semiclassical VUU limit. To this aim we show in Fig. 4 the time evolution of the quadrupole moment in momentum space,

$$Q_2^P(t) = \frac{4}{(2\pi)^3} \int d^3r d^3p (2p_z^2 - p_x^2 - p_y^2) f(\mathbf{r}, \mathbf{p}; t), \quad (42)$$

where $f(\mathbf{r}, \mathbf{p}; t)$ results from the VUU equation (31) in either the mean-field limit (denoted by Vlasov) or the VUU limit including the on-shell two-body collisions (VUU). As in case of the quantal approaches there is only a minor damping in the Vlasov case whereas a rapid decay of $Q_2^P(t)$ is seen in the VUU limit. Unfortunately, no precise temperature T can be attributed to the semiclassical calculations due to numerical reasons since the testparticle method involves numerical fluctuations in the collective coordinate as well as in the total energy. From the size of the numerical fluctuations we estimate the 'excitation' temperature to be in the order of 3-5 MeV.

Since the VUU approach includes only on-shell particle-particle collisions and leaves out particle-hole interactions, which are important for the damping of shape vibrations [31], it yields a moderate damping in between the limits TDHF and TDDM. From the height and position of the maxima (and minima) we can extract the average collective frequency Ω in all cases as well as an average friction constant Γ_Q using $Q(t) \sim \exp(-\Gamma_Q t/2\hbar)$. The latter quantity is shown in Fig. 5 for initial nuclear temperatures T of 0, 1, 2, 3, 4, 5, and 6 MeV for TDHF and TDDM where the error bars indicate the uncertainty of extraction from the time-dependent signal $Q(t)$ or $\dot{Q}(t)$.

The actual values are found to be approximately independent on temperature for TDHF, whereas the damping drops with T for TDDM. Fig. 5, furthermore, shows that the damping achieved in TDHF compares well with the semiclassical Vlasov limit for $T \simeq 3 - 5$ MeV and the additional damping introduced by collisions in VUU only provides about half of the friction obtained from TDDM at low temperature ($T \approx 0$). This result indicates the essential role played by the particle-hole correlations (long-range correlations) in the damping of shape and surface vibrations. As discussed in [7, 35] a sizeable damping arises from the particle-hole (p-h) interaction matrix $H_{\alpha\beta\alpha'\beta'}$ (14) that is not considered in the limit with nonperturbative p-p and h-h scattering (e.g. VUU like models or in Ref. [33]).

The actual magnitude of $\Gamma_Q \approx 5 - 6 \cdot 10^{21} \text{s}^{-1}$ at $T \approx 0$ from TDDM compares well with the friction constant extracted experimentally from the width of the GQR for ^{40}Ca and indicates the importance of p-h residual matrix elements.

The dropping of the width Γ_Q with temperature for TDDM in case of isoscalar quadrupole motion can be attributed to the fact that the long-range correlations de-

crease in magnitude with temperature. In order to demonstrate this dependence we show in Fig. 6 the dependence of the correlation energy on temperature T which in magnitude decreases by a factor of 2 from $T = 0$ to $T = 6$ MeV. Thus the 'long-range correlations melt with temperature' and the width of the giant quadrupole resonances should decrease with T . This is opposite to the role of on-shell 2-body collisions which are blocked in the VUU limit at $T=0$ and increase with phase space as $\sim T^2$. Off-shell collisions allow for a faster increase of phase-space with temperature as demonstrated in Ref. [33], however, the functional dependence of the collisional width depends crucially on the multipolarity of the mode. Thus dominantly the particle-hole correlations induced by (14) generate sizeable density fluctuations at low temperature T which lead to a coupling of different collective modes and a redistribution of their strength.

3.2 Dispersion of giant quadrupole motion

In the quantum theories the dispersion of one-body operators can be evaluated explicitly and the effect of 2-body correlations on these 2-body operators can be analyzed in detail. We note that a collective mass parameter can be extracted from the calculations via

$$E_{coll} \approx \frac{M_Q}{2} \langle \dot{Q} \rangle_{max}^2 \approx \frac{M_Q}{2} \Omega^2 \langle Q \rangle_{max}^2 \quad (43)$$

and leads to $M_Q \approx 2.0 MeV / (fm^2 c^2)$ which is practically equivalent with the value of the direct calculation from Eq. (18). The calculated dispersions $\sigma_Q^2(t)$ and $\sigma_{\dot{Q}}^2(t)$ according to (22) are found to oscillate in phase with the quadrupole moment $\langle Q \rangle(t)$ or $\langle \dot{Q} \rangle(t)$ (cf. Fig.7). When using the same initial conditions $\sigma_Q^2(t=0)$ and $\sigma_{\dot{Q}}^2(t=0)$ as well as the collective frequency Ω and $\gamma_Q = \Gamma_Q$ from the TDDM calculations, the quantum harmonic oscillator (QHO, Eqs. (33)-(35)) gives comparable solutions for $\sigma_Q^2(t)$ and $\sigma_{\dot{Q}}^2(t)$ which, however, are damped out faster in time (dotted lines in Fig. 7). In case of TDDM or TDHF the solutions still oscillate around some average value.

The asymptotic values of σ_Q^2 and $\sigma_{\dot{Q}}^2$ (for $t \rightarrow \infty$) are obtained by averaging over the final time interval (typically for $t \geq 7.5 \cdot 10^{-22} sec$) and shown in Fig. 8 as functions of the initial temperature T . Whereas σ_Q^2 and $\sigma_{\dot{Q}}^2$ only slightly varies with temperature for the QHO, the variation with T is more pronounced for TDDM (solid lines) and especially TDHF (dashed lines), which reflect the intrinsic dynamics. Thus model studies based on the QHO equations of motion should be taken with care especially at high temperature [43].

The product $M_Q^2 \sigma_Q^2 \sigma_{\dot{Q}}^2$ according to (20) must obey the uncertainty relation in all quantum mechanical approaches. This is demonstrated in Fig. 9 for TDDM (solid line), TDHF (dashed line) and the QHO (dotted line) as a function of temperature T . Note, that $\hbar^2 \approx 0.4 (MeV \cdot 10^{-21} s)^2$.

Since $\frac{1}{2} M_Q \sigma_Q^2$ together with the potential energy $\frac{1}{2} M_Q \Omega^2 \sigma_Q^2$ should reflect the equipartition theorem in case of damped harmonic motion, [23]

$$E_Q(T) = \frac{1}{2} M_Q \sigma_Q^2 + \frac{1}{2} M_Q \Omega^2 \sigma_Q^2 = E_Q(0) + T, \quad (44)$$

and thus be a linear function of the temperature T according to Eq. (44), we have plotted

$$\Delta E_Q(T) = E_Q(T) - E_Q(0) \quad (45)$$

in Fig. 10 for all three cases. Here only the full two-body theory TDDM follows equipartition for $T \geq 1$ MeV, i.e. $\Delta E_Q(T) = T$, whereas TDHF as well as the QHO significantly overestimate or underestimate the dash-dotted line, respectively. The off-set of ≈ 1 MeV for TDDM at $T = 0$ so far is not understood.

4 Specific heat, entropy and free energy

Apart from the crucial role of long-range correlations in the damping of the collective quadrupole motion demonstrated in Section 3, the two-body correlations are expected to modify also the thermodynamic properties relative to a mean-field approach. To investigate this question we calculate the total energy of our test-nucleus ^{40}Ca (without any collective excitation) as a function of the initial temperature from $T=0$ to $T=6$ MeV. We note that due to two-body correlations the binding energy is lowered by ≈ 20 MeV (i.e. -382 MeV) for TDDM as compared to TDHF (-362 MeV).

In Fig. 11 we show the total energy for TDDM (full squares; shifted by 20 MeV) and TDHF (full circles) as a function of temperature (upper part) as well as the specific heat (27) (lower part). The total energy increases slightly faster with T for TDDM as for TDHF due to a decrease in the correlation energy with T (cf. Fig. 6). Whereas the increase of the energy is monotonous for TDHF, there is a more rapid variation of the total energy for TDDM at $T \approx 4$ MeV. This is seen more clearly in the specific heat (lower part), where C_V shows a sudden bump around $T \approx 4$ MeV, whereas the specific heat is flat as a function of T for TDHF.

Since conventionally maxima in the specific heat are attributed to phase transitions, where the fluctuations in energy become very large, we have evaluated the quantity $\langle H^2 \rangle - \langle H \rangle^2$ according to (30). As seen from Fig. 12 the fluctuations in the total energy also show a bump at $T \approx 4$ MeV for TDDM (solid triangles) whereas they stay rather flat for TDHF (open circles) in this temperature region.

The origin of this bump is not due to a rapid change of the correlation energy (cf. Fig. 6) but reflects the melting of single-particle effects in case of TDDM. This is demonstrated in Fig. 13 where we show the single-particle density $\rho(x=y=0; z)$ as a function of the coordinate z for temperatures from $T=0$ to $T=6$ MeV (upper part) as well as the single-particle potential (lower part). The pronounced maxima (for $z \approx 0$) in case of low temperature $T \leq 3$ MeV no longer appear for $T \geq 4$ MeV contrary to the case of TDHF. We attribute this behaviour to the melting of shell structure by the two-body correlations in case of TDDM which is accompanied by a larger specific heat as well as larger fluctuations in the total energy (cf. Figs. 11 and 12).

We finally note that the role of two-body correlations also shows up in the entropy S (28) and the free energy F (29) of the nucleus. The latter two quantities are displayed in Fig. 14 as a function of temperature for TDDM and TDHF. Whereas the two-body correlations lead to a decrease of the free energy F relative to the mean-field result,

they enhance the entropy of the system due to a stronger dynamical mixing of single-particle configurations (Slater-determinants). However, the relative changes turn out to be quite moderate except for a shift of the free energy by ≈ 20 MeV for TDDM due to the correlation energy.

5 Summary and discussion

In this work we have presented microscopic calculations for the nucleus ^{40}Ca within a nonperturbative two-body correlation approach which superseeds TDHF as well as the 'traditional' VUU model [3, 4] by including explicit p-h interactions as well as off-shell collision processes to all orders. Note that more recent extensions of mean-field theory [33, 42] include off-shell collisions, however, are still restricted to the Born approximation.

By studying the decay of collective quadrupole excitations we have extracted transport coefficients for friction and diffusion and analyzed the fluctuation properties of the theory which fulfills the equipartition theorem for the fluctuations in the collective velocity (for $T \geq 1$ MeV) contrary to the mean-field limit TDHF. This study has also shown the essential role played by the particle-hole (long-range) correlations in the damping of shape and surface vibrations in nuclei at lower temperature whereas for $T \geq 3-4$ MeV the particle-particle collisions take over and the system might be conveniently described within the semiclassical VUU limit. The latter phenomena is due to a decrease of the correlation energy with temperature and an increase with phase-space of on-shell two-body collisions with T .

The temperature dependence of the entropy S and the free energy F is found not to be modified substantially due to two-body correlations relative to the mean-field limit. However, a small bump in the specific heat C_V and in the fluctuations in energy shows up for $T \approx 4$ MeV, which does not appear in mean-field theory. We attribute this effect to a melting of shell structure due to two-body correlations.

In view of the detailed microscopic analysis we expect that nucleus-nucleus collisions above 20 A MeV should be adequately described in the semiclassical VUU limit as far as stopping power and single-particle observables are concerned. Multifragmentation phenomena, however, might require the dynamics of long-range correlations [36, 49] especially at low nuclear density. Mean-field dynamics here provide a glance at the complexity of the shape evolution [50, 51] but should not be adequate to describe nuclear condensation phenomena or the growth of instabilities according to the analysis in this work. First steps in exploiting Eqs. (1) - (4) for the description of nucleus-nucleus collisions have been made in Ref. [52].

References

- [1] A. A. Abrikosov, L. P. Gorkov and I. E. Dzyaloshinski, *Quantum field theoretical methods in statistical physics*, (Pergamon, Oxford,1965)

- [2] A. B. Migdal, *Theory of finite Fermi systems and application to atomic nuclei*, (Wiley Interscience, New York, 1967)
- [3] G. F. Bertsch and S. Das Gupta, Phys. Rep. 160 (1988) 189
- [4] W. Cassing, V. Metag, U. Mosel, and K. Niita, Phys. Rep. 188 (1990) 363
- [5] A. Bonasera, F. Gulminelli, and J. Molitoris, Phys. Rep. 243 (1994) 1
- [6] J. Wambach, Rep. Prog. Phys. 51 (1988) 989; S. Drozdz, S. Nishizaki, J. Speth, and J. Wambach, Phys. Rep. 197 (1990) 1
- [7] F.V. De Blasio, W. Cassing, P. F. Bortignon, R. A. Broglia, and M. Tohyama, Phys. Rev. Lett. 68 (1992) 1663
- [8] S. Ayik and C. Grégoire, Phys. Lett. B212 (1988) 269; Nucl. Phys. A513 (1990) 187
- [9] J. Randrup and B. Remaud, Nucl. Phys. A514 (1990) 339
- [10] G. F. Burgio, Ph. Chomaz and J. Randrup, Nucl. Phys. A529 (1991) 157; Phys. Rev. Lett. 69 (1992) 885
- [11] J. Randrup, Nucl. Phys. A545 (1992) 47c
- [12] S. Ayik, E. Suraud, M. Belkacem, and D. Boilley, Nucl. Phys. A545 (1992) 59c
- [13] P. G. Reinhard and E. Suraud, Nucl. Phys. A545 (1992) 59c; Ann. of Phys. 216 (1992) 98
- [14] A. Bonasera, F. Gulminelli, and P. Schuck, Nucl. Phys. A545 (1992) 71c
- [15] Ph. Chomaz, G.F. Burgio, and J. Randrup, Nucl. Phys. A540 (1992) 227
- [16] Y. Abe, S. Ayik, P. G. Reinhard, and E. Suraud, Phys. Rep. 275 (1996) 49
- [17] M. Germain et al., Phys. Lett. B437 (1998) 19
- [18] T. Maruyama, A. Onishi and H. Horiuchi, Phys. Rev. C45 (1992) 2355
- [19] A. Bracco et al., Nucl. Phys. A519 (1990) 47c
- [20] G. Enders et al., Phys. Rev. Lett. 69 (1992) 249
- [21] J. J. Gaardhoje, Annu. Rev. Nucl. Part. Sci. 42 (1992) 483
- [22] E. Ramakrishan et al., Phys. Rev. Lett. 76 (1996) 2025; Phys. Lett. B383 (1996) 252
- [23] W. Cassing and W. Nörenberg, Nucl. Phys. A401 (1983) 467
- [24] P. F. Bortignon, A. Bracco, D. M. Brink, and R. A. Broglia, Phys. Rev. Lett. 67 (1991) 3360

- [25] Ph. Chomas, M. Di Toro and A. Smerzi, Nucl. Phys. A563 (1993) 509
- [26] A. Smerzi, M. Di Toro and D. M. Brink, Phys. Lett. B320 (1994) 216
- [27] C. Toepffer and P.-G. Reinhard, Ann. Phys. 181 (1988) 1
- [28] K. Gütter, P.-G. Reinhard, K. Wagner, and C. Toepffer, Ann. Phys. 225 (1993) 339
- [29] M. Di Toro, V. M. Kolomietz, and A. B. Larionov, nucl-th/9807070
- [30] P. F. Bortignon, M. Braguti, D. M. Brink et al., Nucl. Phys. A583 (1995) 101c
- [31] G.F. Bertsch, P.F. Bortignon, and R.A. Broglia, Rev. Mod. Phys. 55 (1983) 287
- [32] N. D. Dang, K. Tanabe and A. Arima, RIKEN-AF-NP-285, 1998; RIKEN-AF-NP-296, 1998
- [33] D. Lacroix, Ph. Chomaz and S. Ayik, Phys. Rev. C58 (1998) 2154
- [34] M. Tohyama and M. Gong, Z. Phys. A332 (1989) 269; M. Gong and M. Tohyama, Z. Phys. A335 (1990) 153
- [35] M. Gong, M. Tohyama and J. Randrup, Z. Phys. A335 (1990) 153
- [36] W. Cassing, A. Peter and A. Pfitzner, Nucl. Phys. A561 (1993)133
- [37] S. Ayik and J. Randrup, Phys. Rev. C50 (1994) 2947
- [38] S. J. Wang and W. Cassing, Ann. Phys. 159 (1985) 328
- [39] W. Cassing and S. J. Wang, Z. Phys. A328 (1987) 423; Z. Phys. A337 (1990) 1
- [40] W. Cassing and A. Pfitzner, Z. Phys. A337 (1990) 175
- [41] W. Cassing and A. Pfitzner, Z. Phys. A342 (1992) 161
- [42] D. Lacroix, Ph. Chomaz and S. Ayik, *nucl-th/9902050*
- [43] W. Wen, P. Chau Huu-Tai, D. Lacroix, Ph. Chomaz, and S. Ayik, Nucl. Phys. A637 (1998) 15
- [44] P. Bonche, S. E. Koonin, and J. W. Negele, Phys. Rev. C13 (1976) 1226
- [45] A. Pfitzner, W. Cassing, and A. Peter, Nucl. Phys. A577 (1994) 753
- [46] A. Peter, W. Cassing, J. M. Häuser and A. Pfitzner, Nucl. Phys. A573 (1994) 93
- [47] W. Cassing and E. L. Bratkovskaya, Phys. Rep. 308 (1999) 65
- [48] L. Lapikas, Nucl. Phys. A553 (1993) 297c
- [49] H. Heiselberg, C. J. Pethick, and D. G. Ravenhall, Nucl. Phys. A519 (1990) 279c

- [50] C. Jung, W. Cassing, U. Mosel, and R. Y. Cusson, Nucl. Phys. A477 (1988) 256
- [51] D. Lacroix and Ph. Chomaz, Nucl. Phys. A641 (1998) 107; Phys. Rev. C58 (1998) 1604
- [52] Jian-Ye Liu, Shun-Jin Wang et al., Nucl. Phys. A604 (1996) 341

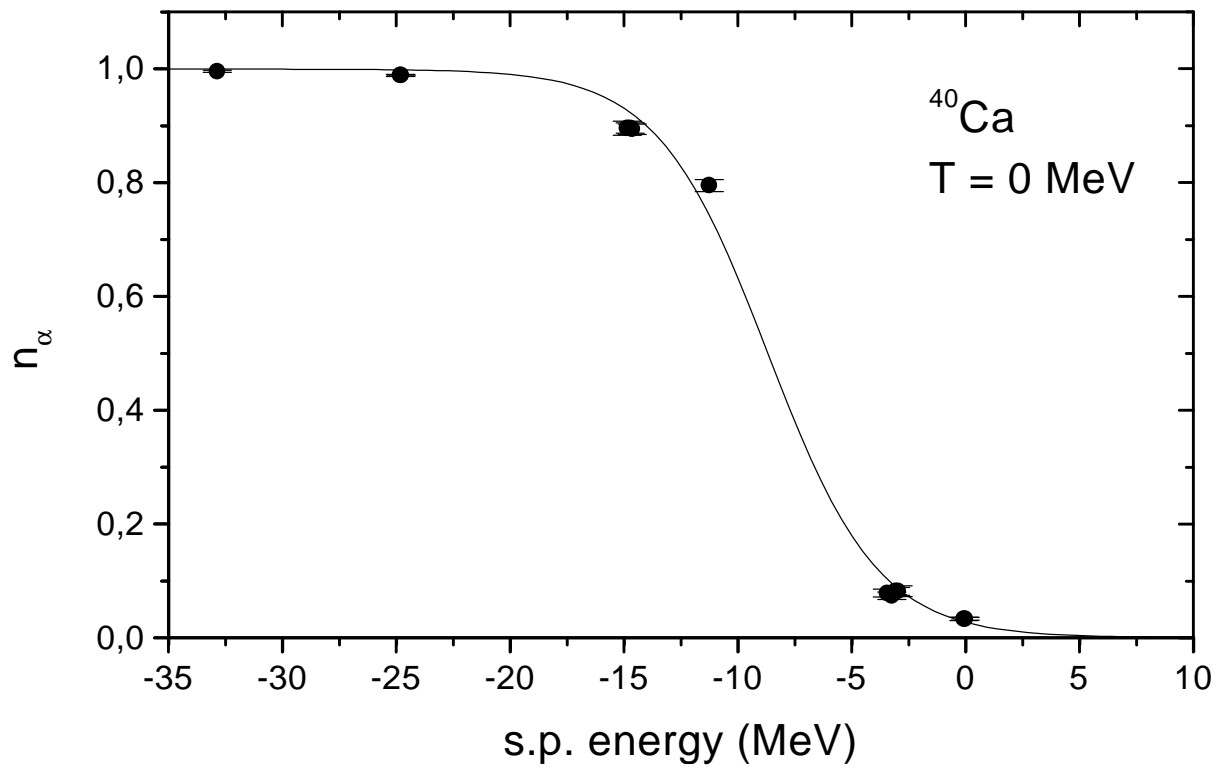


Fig. 1: The time averaged occupation numbers n_α for ^{40}Ca as a function of the s.p. energies ϵ_α at $T = 0$ MeV in the limit TDDM.

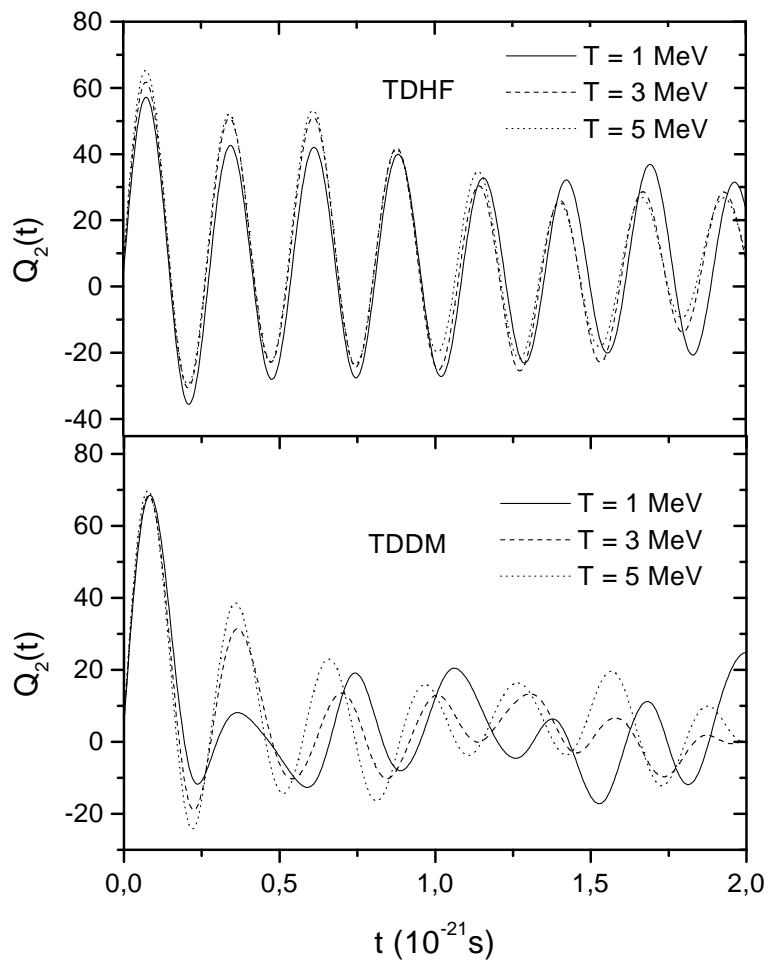


Fig. 2: Time dependence of the quadrupole moment $Q_2(t) \equiv Q(t)$ for an isoscalar excitation of ^{40}Ca of 20 MeV in the limits TDHF (upper part) and TDDM (lower part) at initial temperatures of 1,3, and 5 MeV.

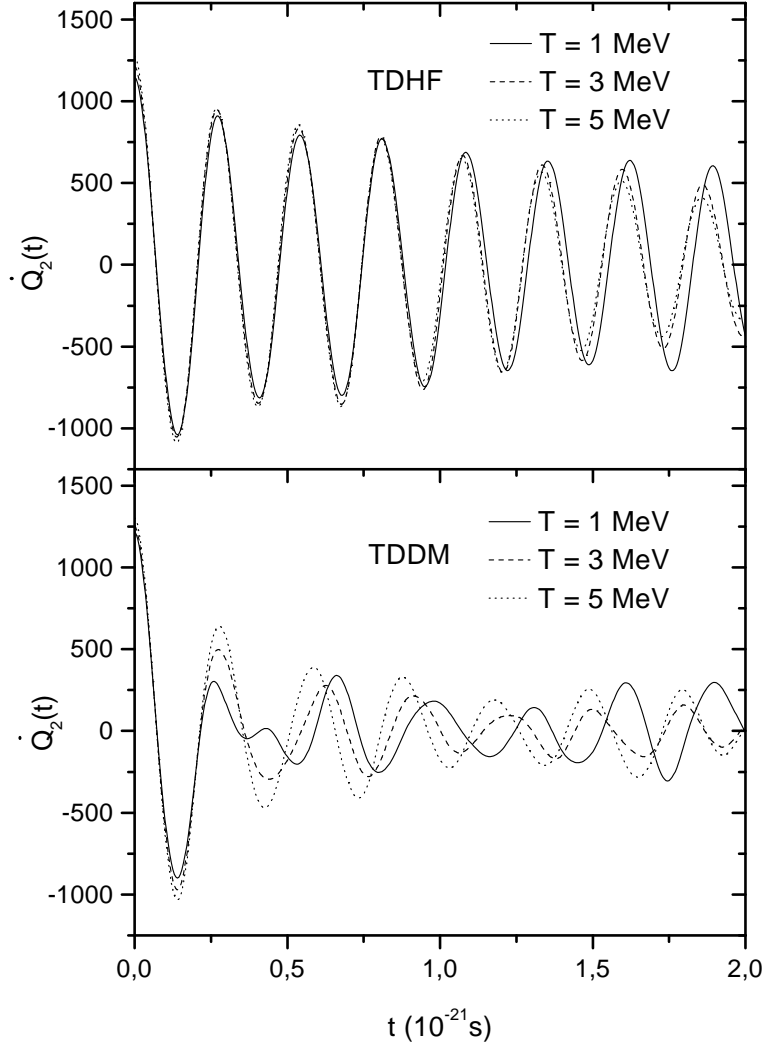


Fig. 3: Time dependence of the quadrupole velocity $\dot{Q}_2(t) \equiv \dot{Q}(t)$ for an isoscalar excitation of ^{40}Ca of 20 MeV in the limits TDHF (upper part) and TDDM (lower part) at initial temperatures of 1, 3, and 5 MeV.

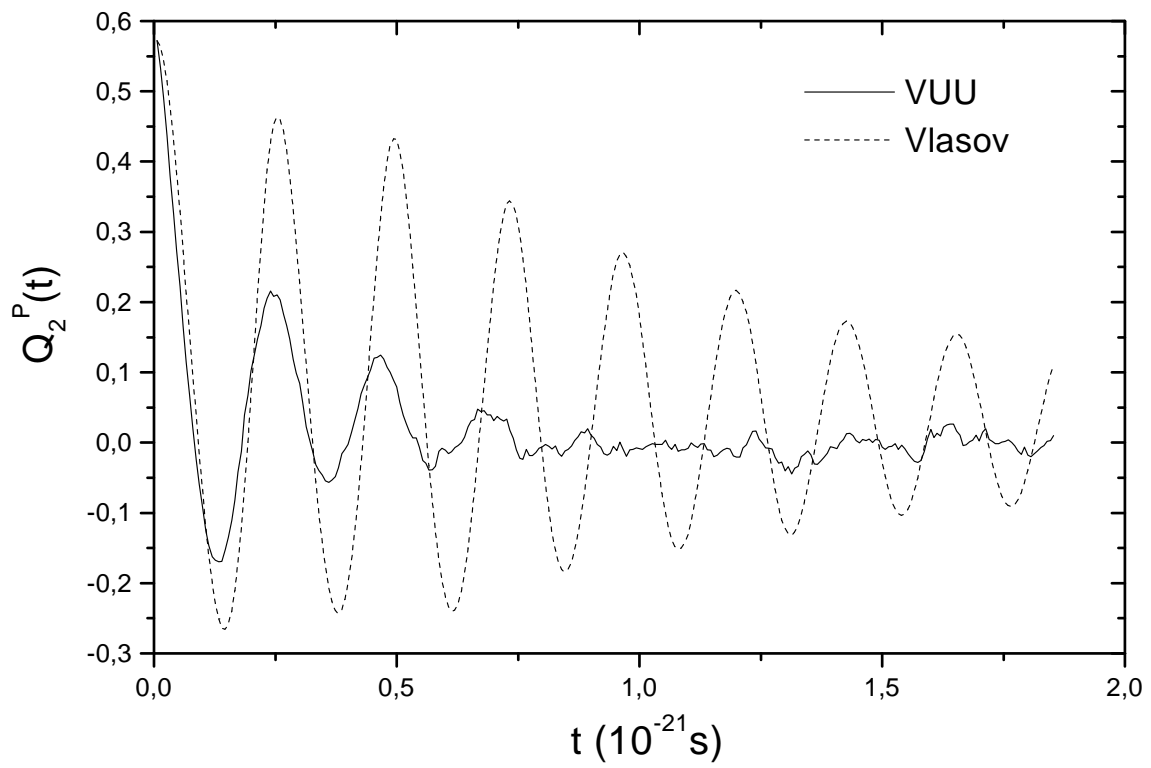


Fig. 4: Time evolution of the quadrupole moment in momentum space (42) in the limits VUU (solid line) and Vlasov (dashed line)

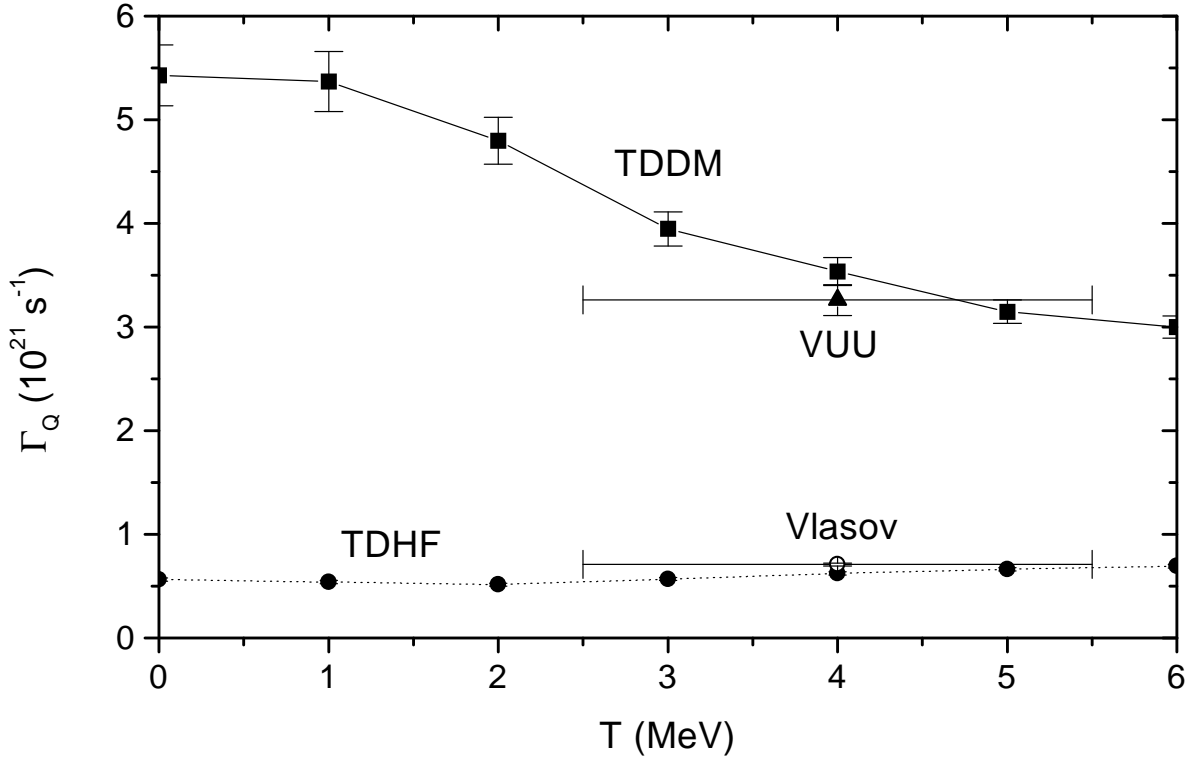


Fig. 5: Extrapolated values for the friction coefficient Γ_Q as a function of the initial temperature T in the limits TDDM, TDHF, VUU, and Vlasov.

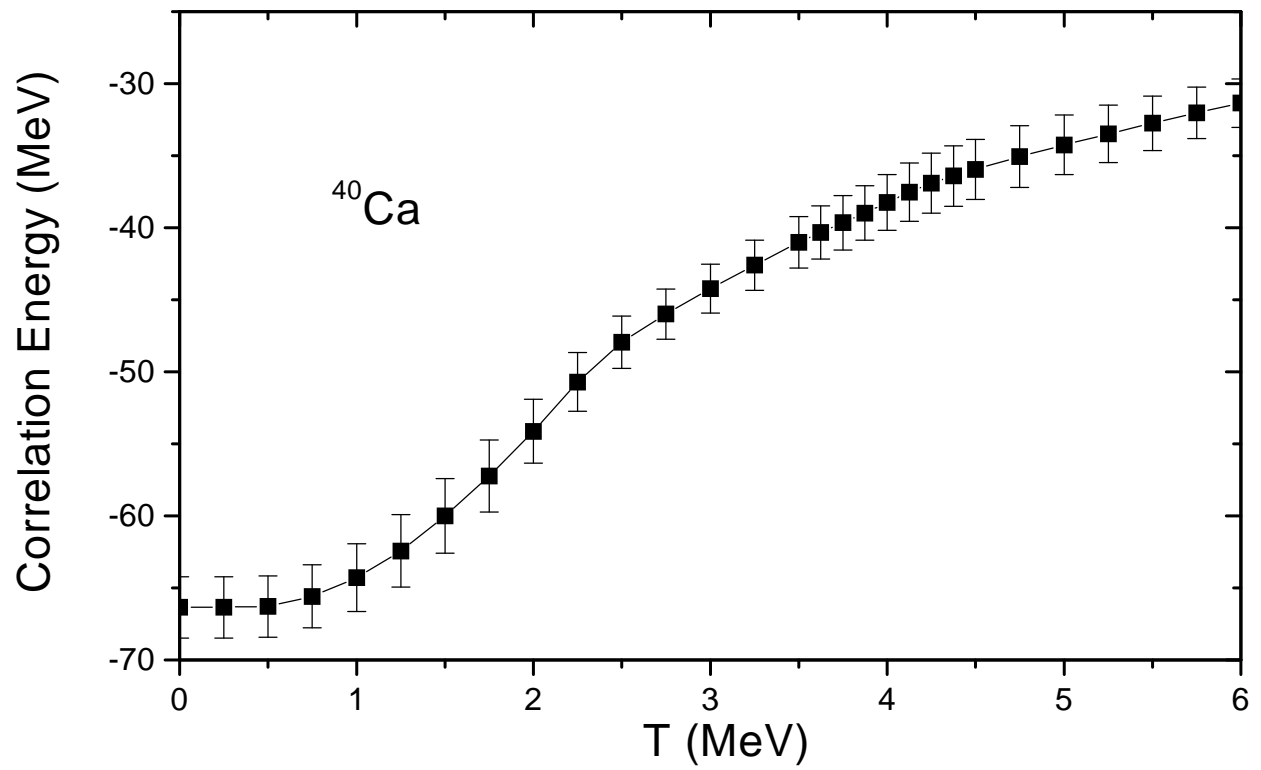


Fig. 6: The correlation energy for ^{40}Ca in the limit TDDM as a function of temperature T .

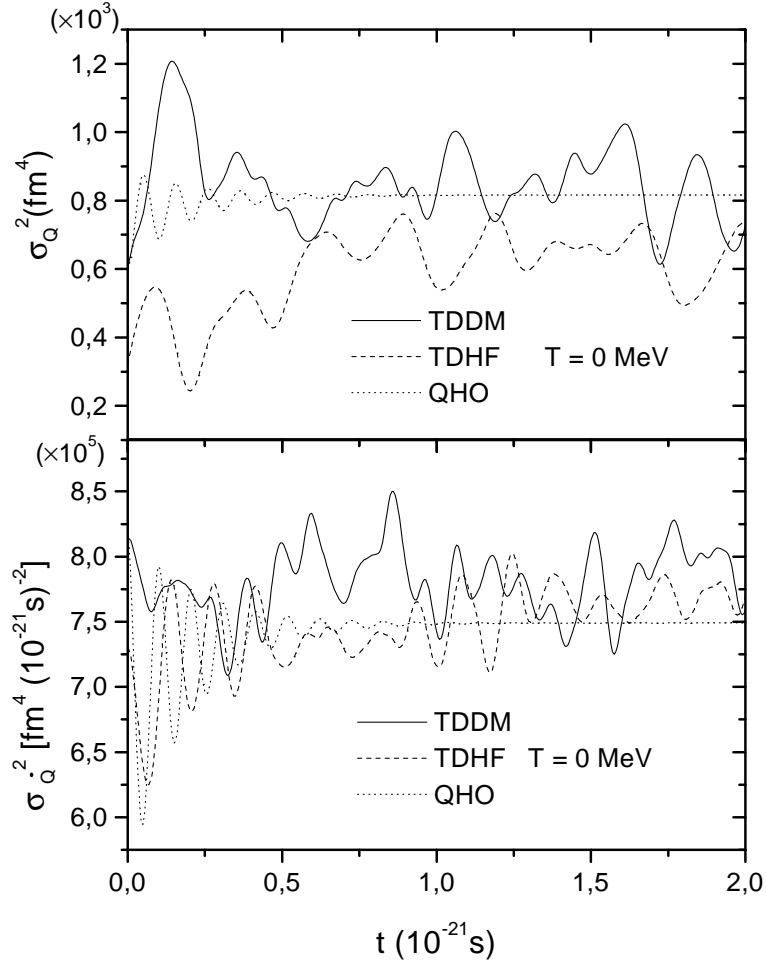


Fig. 7: The fluctuations $\sigma_Q^2(t)$ (upper part) and $\sigma_Q^2(t)$ (lower part) for ^{40}Ca excited collectively by 20 MeV in the limit TDDM (full lines) and TDHF (dashed line) in comparison to the results from the damped quantum harmonic oscillator (QHO; dotted lines).

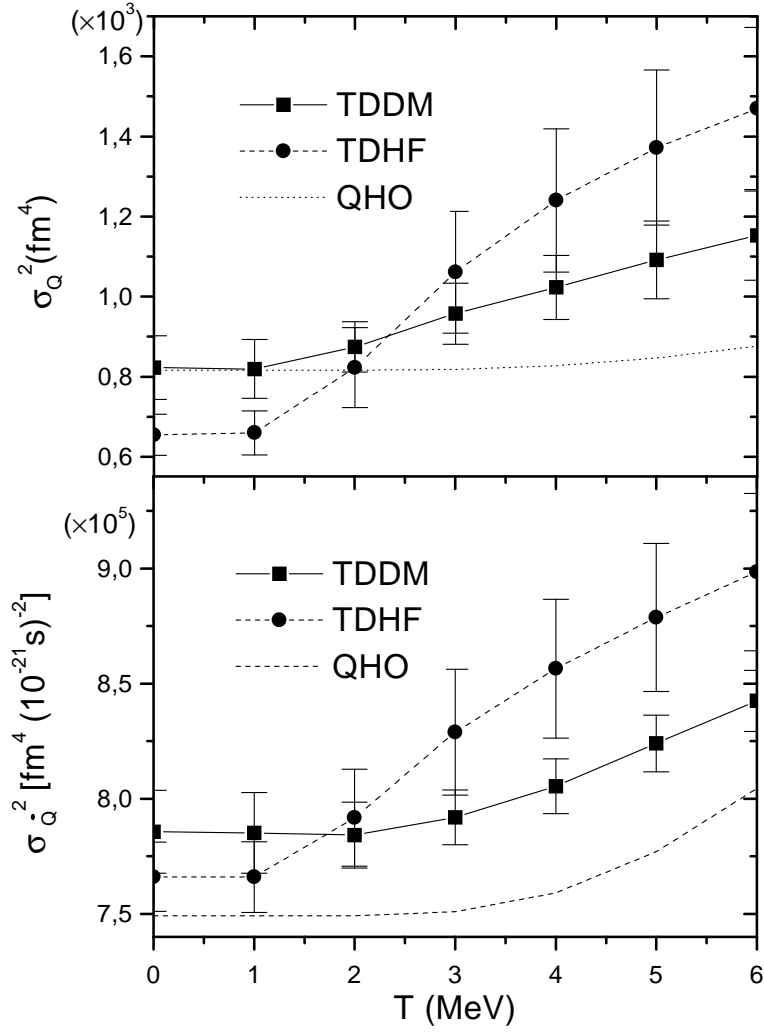


Fig. 8: Asymptotic fluctuations in the quadrupole degree of freedom $\sigma_Q^2(\infty)$ (upper part) and in the quadrupole velocity $\sigma_{\dot{Q}}^2(\infty)$ (lower part) in the limits TDDM, TDHF and the quantum harmonic oscillator QHO.

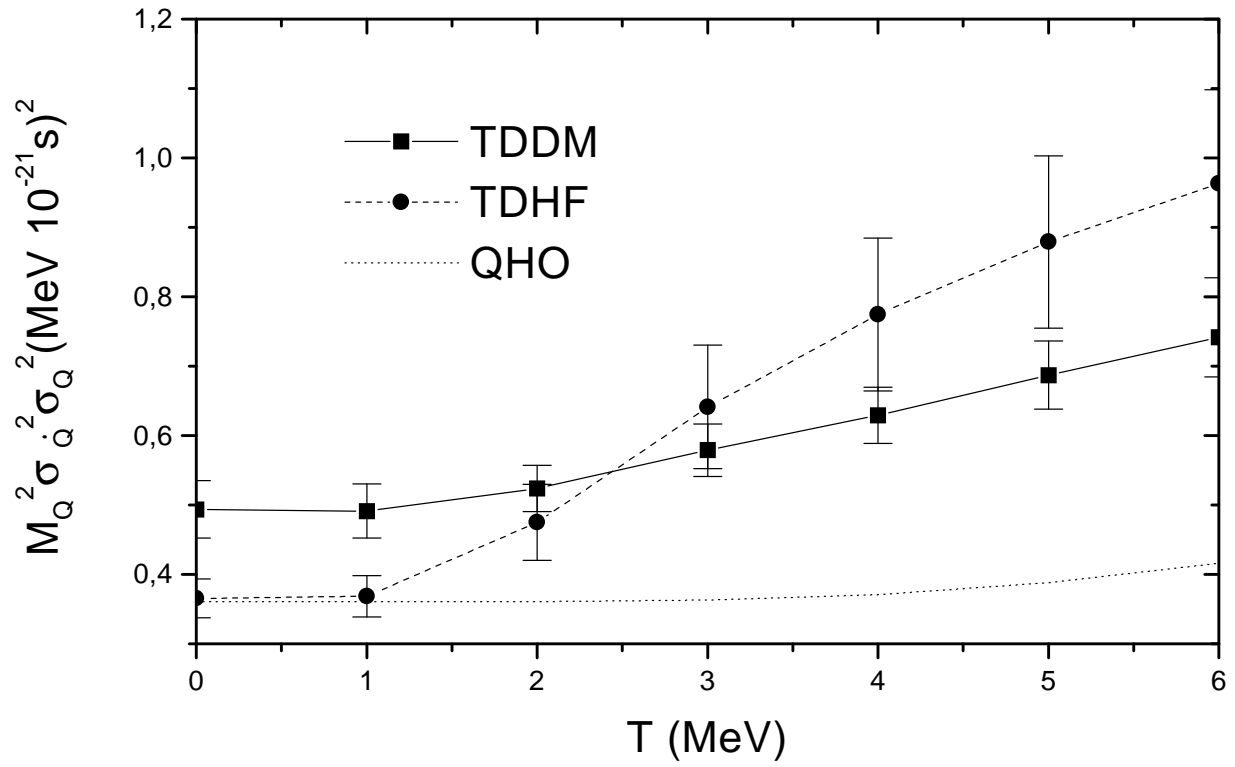


Fig. 9: Test of the uncertainty relation for TDDM (solid line), TDHF (dashed line) and the QHO (dotted line) as a function of T .

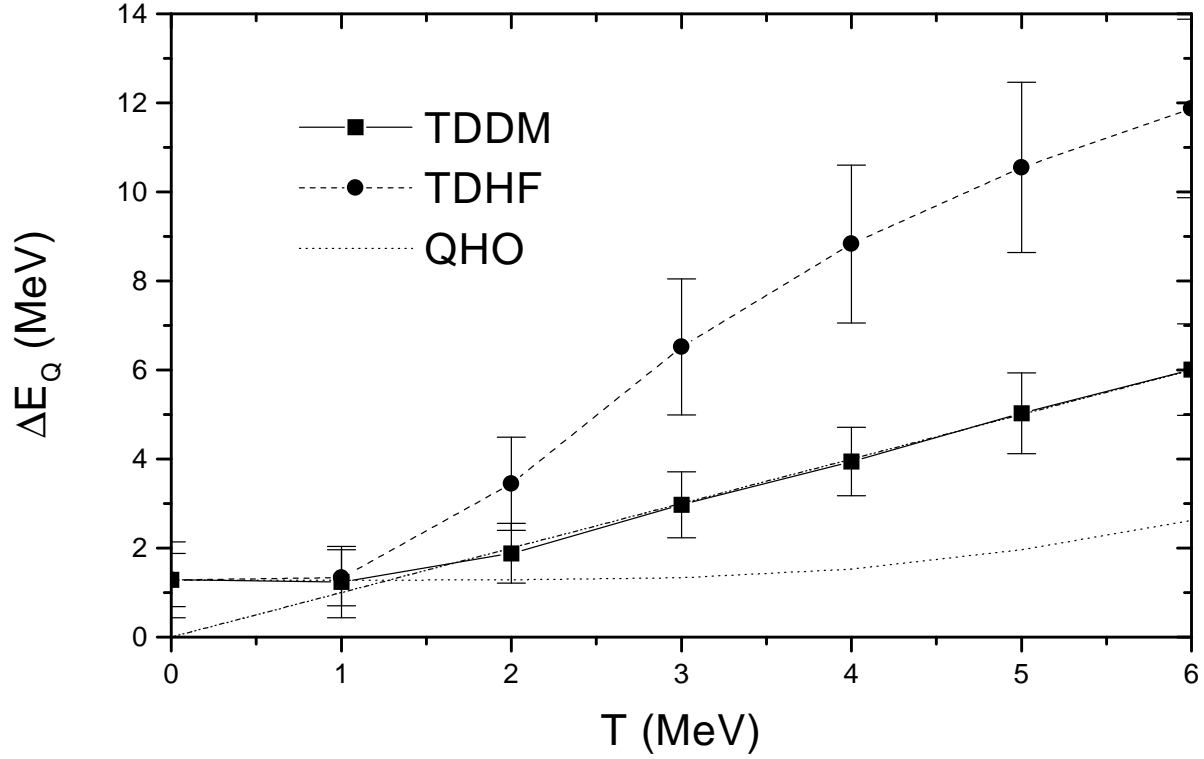


Fig. 10: Test of the equipartition relation for $\Delta E_Q(T)$ (45) (straight dash-dotted line) for the collective fluctuations as a function of temperature in the limits TDDM, TDHF and the quantum harmonic oscillator QHO.

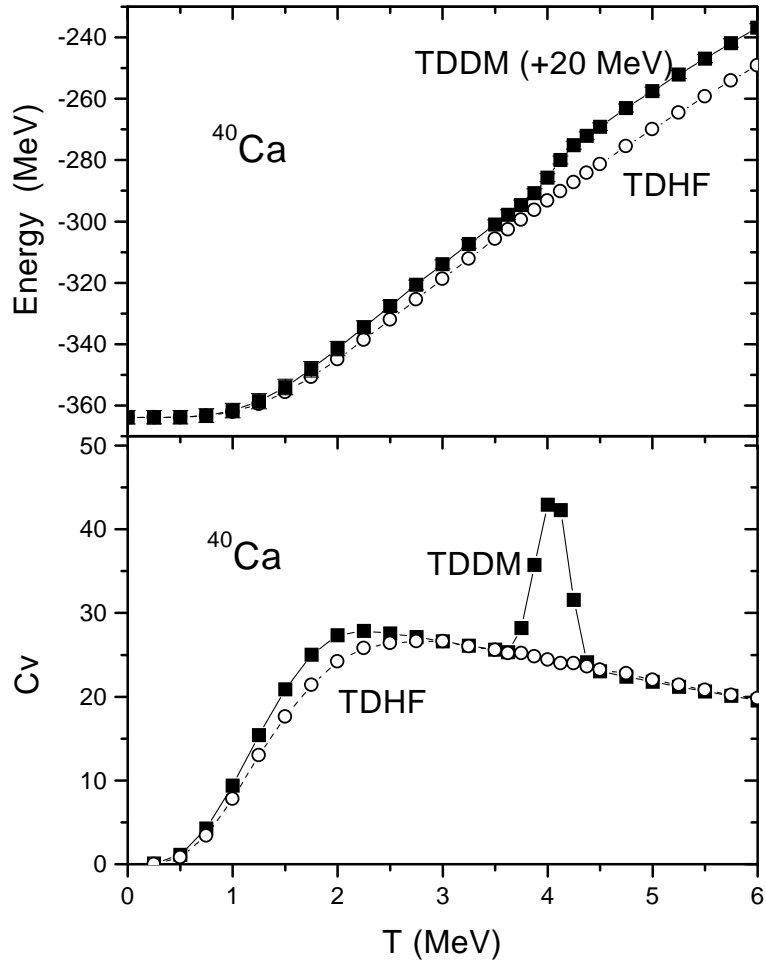


Fig. 11: The total energy (upper part) and the specific heat (27) (lower part) of the system ^{40}Ca as a function of temperature in the limits of TDHF (open circles) and TDDM (full squares).

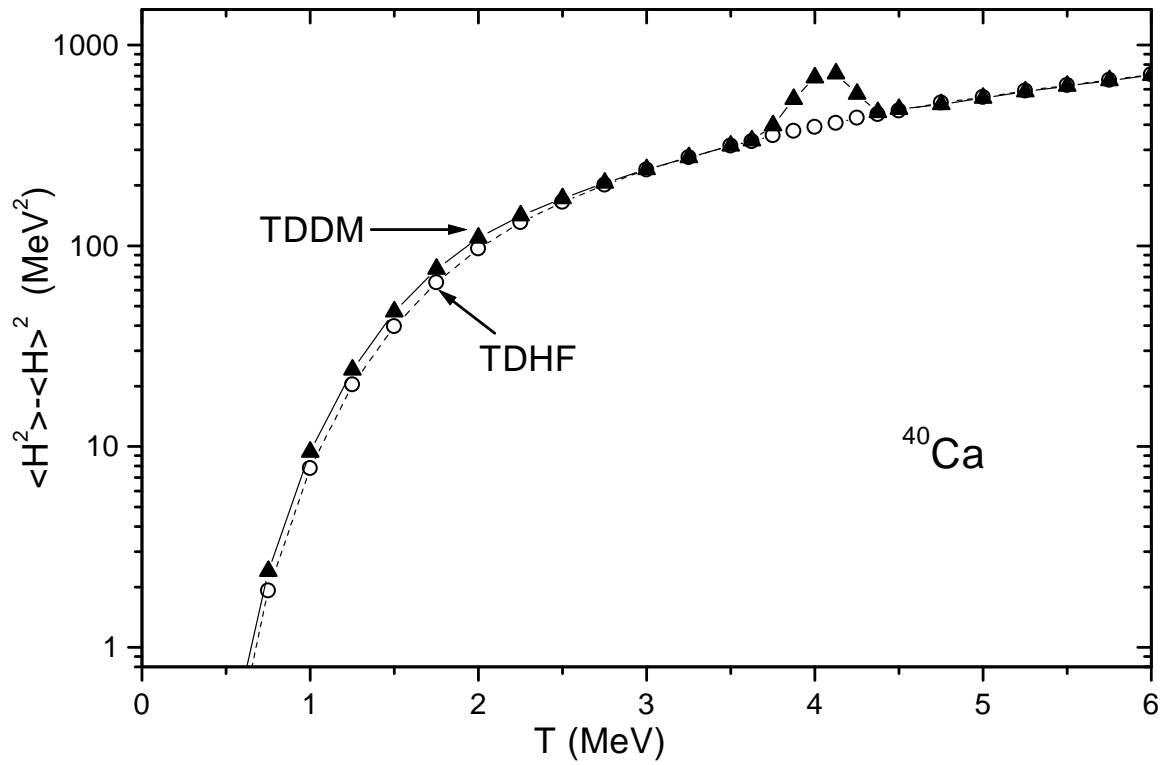


Fig. 12: The fluctuation in energy (30) of the system ^{40}Ca as a function of temperature in the limits of TDHF (open circles) and TDDM (full triangles).

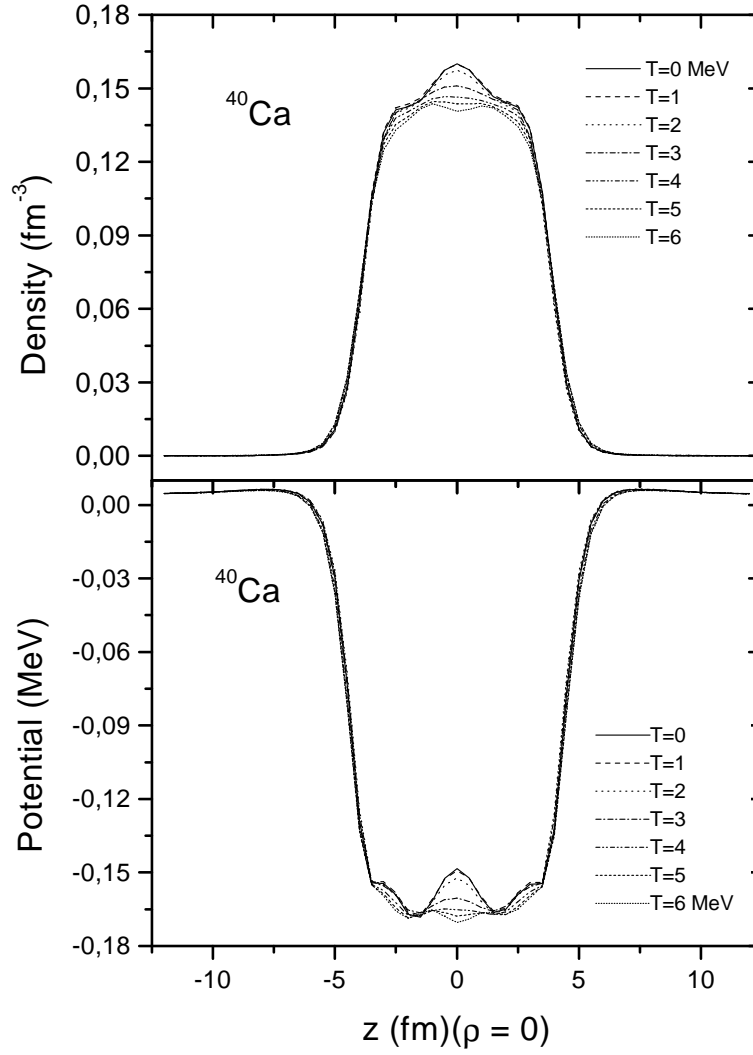


Fig. 13: The nuclear density (upper part) and the single-particle potential (lower part) for ^{40}Ca as a function of the coordinate z for temperatures $T = 1, 2, 3, 4, 5, 6$ MeV in the limit TDDM.

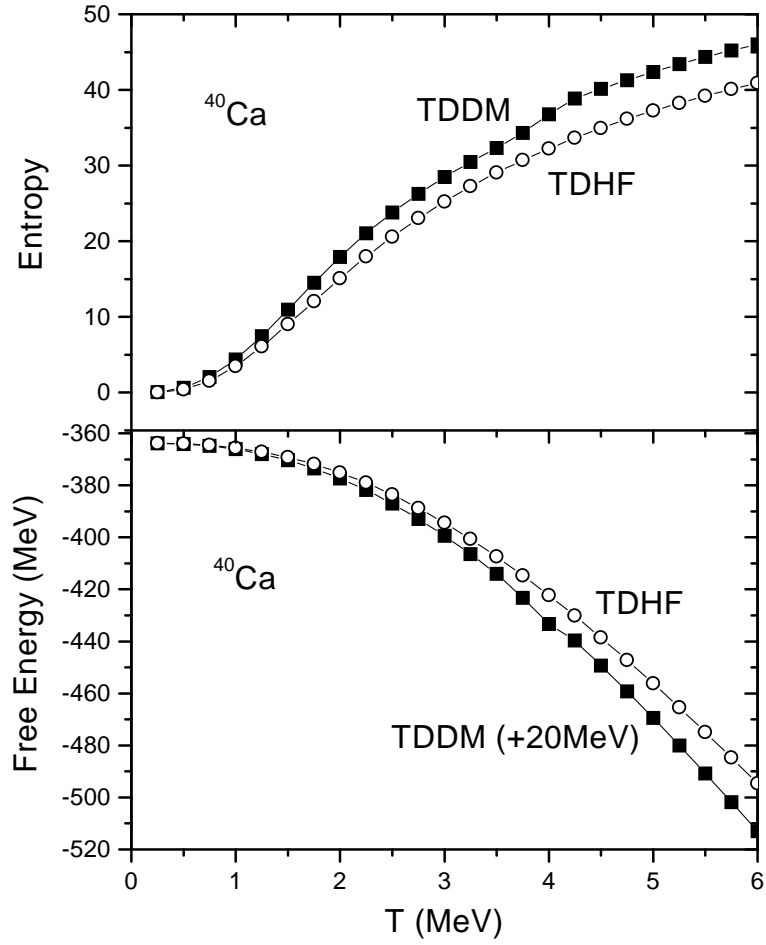


Fig. 14: The entropy S (28) (upper part) and free energy F (29) (lower part) for ^{40}Ca as a function of temperature for TDDM and TDHF.